Lett. **28**, 401 (1972); T. S. Murtaugh and W. P. Reinhardt, J. Chem. Phys. 57, 2129 (1972).
[14]R. G. Newton, Ref. 6, p. 543.
[15]See, for example, J. R. Taylor, *Scattering Theory* (Wiley, New York, 1972), Chap. 20.
[16]See, for example, the analysis of the singularities of $D(k_1, k_2 \ldots k_l \ldots)$ for coupled superpositions of Yukawa potentials in R. G. Newton, Ref. 6, p. 546.
[17]R. G. Newton, J. Math. Phys. **8**, 2347 (1967).
[18]S. C. Pieper, Jon Wright, and L. Schlesinger, Phys. Rev. D **3**, 2419 (1971).

PHYSICAL REVIEW A VOLUME 8, NUMBER 2 AUGUST 1973

High-Resolution Photodetachment Study of Se^- Ions*

H. Hotop† and T. A. Patterson
Joint Institute for Laboratory Astrophysics, University of Colorado, Boulder, Colorado 80302

W. C. Lineberger‡
Dept. of Chemistry and Joint Institute for Laboratory Astrophysics, University of Colorado, Boulder, Colorado 80302

(Received 22 March 1973)

Photodetachment of Se^- ions is studied in a crossed-beam experiment, in which a 2-keV negative-ion beam is intersected by a pulsed tunable dye laser ($\Delta\lambda \approx 1$–2 Å). The threshold behavior of the photodetachment cross section σ is compatible with Wigner's law $\sigma_L \propto k^{2L+1}$ (k is the magnitude of the momentum of the outgoing electron and L is its orbital angular momentum) over only about 5 meV above threshold in this case ($L = 0$). Some differences are observed for the threshold behavior of transitions terminating in different final states of $Se(^3P_{2,1,0})$. These results are discussed in the light of existing theory. The observation of four of the six possible fine-structure transition thresholds allows us to determine unambiguously the electron affinity (EA) of Se {EA[Se = (16297 ± 2) cm^{-1} ≅ (2.0206 ± 0.0003) eV]} and the spin-orbit splitting between the $^2P_{3/2}$ and $^2P_{1/2}$ states in Se^- [(2279 ± 2) cm^{-1} ≅ (282.6 ± 0.3) MeV]. Comparison of experimental results for this splitting in O^-, S^-, and Se^- is made with predictions from isoelectronic extrapolation. The transition strengths for the various fine-structure transitions are determined and agree well with predictions by Rau and Fano. Finally, the absolute cross section for $Se^-(^2P_{3/2})$ detachment is reported.

I. INTRODUCTION

The energy resolution in photodetachment experiments

$$A^- + h\nu \rightarrow A + e^- \tag{1}$$

has recently been greatly improved to better than 1 meV by use of continuously tunable dye-laser light sources.[1,2] The first such results were reported by Lineberger and Woodward[1] on the photodetachment of S^-. Their measurements not only provided a precise determination of the electron affinity of the sulphur atom but also produced the first reliable verification of the theoretically predicted behavior of the cross section for photodetachment near threshold.

According to the work of Wigner[3] on threshold laws, the leading term of the energy dependence of photodetachment cross sections near threshold is given by

$$\sigma \propto k^{2L+1} \propto E^{(2L+1)/2}, \tag{2}$$

where L is the orbital angular momentum of the detached electron, k the magnitude of the momentum, and E its kinetic energy. In deriving Eq. (2), it is assumed that the long-range forces between the departing electron and the atom (other than the centrifugal potential) fall off faster than $1/r^2$, a condition which is fulfilled for all atoms except $H(n \geq 2)$.[4]

If a p electron is detached, such as in O^-, S^-, or Se^-, the outgoing electron can be in an s or d wave. The theoretical behavior is given by the s-wave contribution $\sigma \propto k$, since the d-wave cross section is suppressed by the centrifugal barrier. One of the more interesting questions to be answered by a high-resolution experiment is, over how large an energy range does Eq. (2) give a satisfactory description of the cross section?

If one were to take a sophisticated point of view, one could argue that no experiment can give that answer because of the finite uncertainties in every measurement. In this sense, the experiment will only provide evidence—more or less clear evidence, depending on the error bars—that the threshold law holds over a certain energy range beyond which deviations become obvious. It would be very desirable, of course, if theory could provide an estimate of the minimum energy range over which the Wigner law is valid, i.e., a good de-

scription of the experimental data. Such estimates can be given on the basis of correction terms to the Wigner law having to do with the influence of the long-range interactions (other than the centrifugal potential) between the detached electron and the final-state atom. Such corrections have been derived by O'Malley[4] for three different cases; we shall discuss this point in more detail later. Unfortunately, it is not possible to give a closed expression for *all* of the correction terms on the basis of long-range parameters only; it may be useful, nevertheless, to estimate only the correction terms that originate from the long-range interactions, e.g., from the electron-induced dipole force. We thus hope to obtain a feeling for where deviations would be expected to become significant (say $\gtrsim 5\%$), since it may very well be that these correction terms are the dominant ones. In the case of S^-, Eq. (2) describes the measured cross section satisfactorily up to about 10–20 meV above threshold. However, the rather small energy differences between the various fine-structure onsets $S^-(^2P_{3/2,1/2}) \rightarrow S(^3P_{2,1,0})$ prevented the study of the individual onsets over larger energy ranges.

For Se the fine-structure splittings are appreciably larger than in S (by almost a factor of 5), and one can study the transitions over a more extended energy range. Since the spin-orbit splitting in Se^- is also about five times larger than in S^- (where it is 482 cm^{-1}), one has the additional advantage that the Se^- ions in the beam, generated in an ion source at about 1500 °K, are preferentially in the ground $Se^-(^2P_{3/2})$ state. The relatively few $Se^-(^2P_{1/2})$ ions in the beam make only a small contribution to the observed photodetachment cross section.

In addition to the question of the threshold behavior of the cross section, there is interest in the relative transition strengths for the various fine-structure onsets, which in S^- have been found to deviate substantially from simple statistical expectations. In the present study, we have also accurately determined the $^2P_{3/2}$-$^2P_{1/2}$ spin-orbit splitting in the Se^- ions; comparison of the splittings for S^- and Se^- with values obtained via isoelectronic extrapolation are made, and the resulting evidence is used to obtain an estimate of this quantity for O^- and Te^-. Since the S^- data[1] were taken, the data-acquisition system has been improved considerably. As a result, the present measurements have better statistics, and more accurate determinations of the transition strengths for the various fine-structure onsets are possible, as well as more detailed studies of the threshold behavior of the cross section.

II. EXPERIMENTAL

A schematic diagram of the apparatus is shown in Fig. 1. The basic idea is to intersect a 2-keV mass-analyzed Se^- beam with the focused output of a pulsed, tunable dye laser and to measure the relative cross section for production of Se neutrals as a function of the laser wavelength. The negative ions are formed in a hot cathode arc discharge source, accelerated, mass analyzed, and focused onto a 15-stage particle multiplier located 20 cm beyond the laser-beam–ion-beam intersection. After passing through the interaction region, but before reaching the multiplier, the ions are electrostatically deflected into a Faraday cup, so that only the neutral atoms, produced by charge strip-

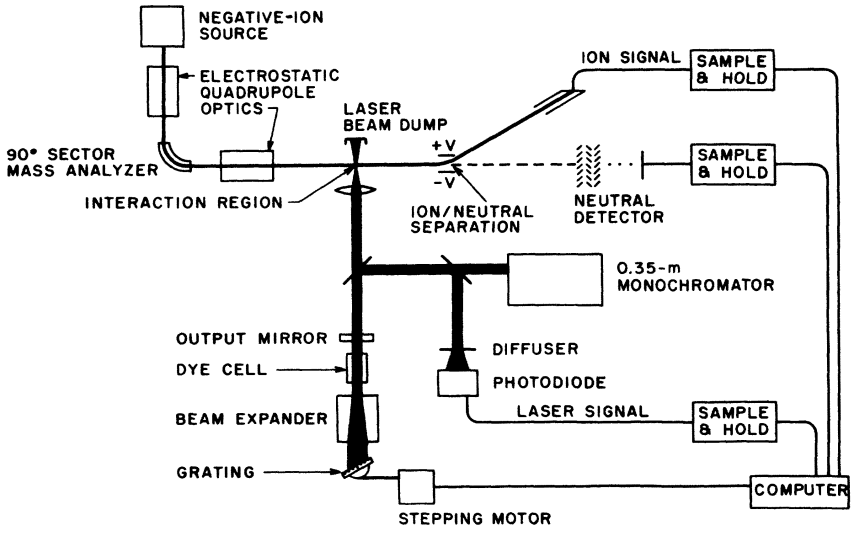

FIG. 1. Schematic diagram of the tunable laser photodetachment apparatus.

ping on the background gas and by laser photodetachment, reach the neutral detector. As a result of the large number of neutrals reaching the multiplier in a short time interval, the detector is operated in a linear, charge-amplifying mode rather than as a particle counter. The following sections discuss the apparatus in greater detail and describe the data acquisition and reduction methods employed.

A. Ion Source and Optics

The Se^- ions are formed in a magnetically confined hot cathode discharge source that has been used in previous negative-ion experiments.[1] The source has been modified by the addition of a stainless-steel crucible attached to the first plasma ring. The crucible is filled with selenium dioxide and a discharge is run in carbon monoxide gas at an estimated pressure of 50 mTorr. At the ~200 °C operating temperature of this electrode, the SeO_2 decomposes, providing a source of Se vapor for the discharge. Typical operating conditions are an arc voltage of 225 V, a discharge current of 25 mA, and a beam energy of 2 keV. Under such conditions, a beam of about 80 nA of Se^- is produced which remains relatively stable for 2–4 h.

Negative ions are extracted from the discharge, accelerated to 2 keV, and focused by means of an electrostatic quadrupole doublet onto the entrance aperture of a 90°-sector magnetic mass spectrometer having a resolution $m/\Delta m$ of about 40. Since the mass filter cannot differentiate between Se^- and SeH^-, care was taken to avoid the introduction of hydrogen-containing gases into the ion source. The OH^- and H^- intensities were down several orders of magnitude from that of Se^-. In addition no onset was seen at the photon energy appropriate[5] for SeH^-. A second quadrupole doublet then focuses the mass-selected ion beam onto the first stage of the multiplier normally used for neutral atom detection. Included in the ion optical system is a small (~5°) deflection just prior to the interaction region. This deflection is adequate to permit spatial separation of the laser-produced neutrals from those produced by charge stripping in the relatively high-pressure region (~10^{-6} Torr) prior to the small deflection. This deflection significantly reduces the noise, since the differentially pumped interaction and neutral detector chambers are at pressures of 10^{-8} Torr.

B. Tunable Laser

In the interaction region, the ion beam is intersected normally by the output of a flashlamp pumped pulsed tunable dye laser. The laser dye cell, located at one focus of an elliptical cavity,[6] is pumped by a linear xenon flashlamp located at the other focus. The laser optical cavity is defined by a partially transmitting mirror and an 1800-lines/mm grating blazed at 5000 Å in first order. A 4× telescope is sometimes used for beam expansion onto the grating. Tuning is accomplished by rotating the grating using a computer-controlled stepping motor. A beam splitter is used to divert a portion of the output to a solid-state photodiode for laser power measurement. Typical flashlamp-pumping energies are 10–15 J. The laser is normally operated at 5 pulses per sec, and produces an output pulse whose time duration is ~0.3 μsec. Five different dyes were required to cover the wavelength region studied (7000–5200 Å); their ranges and output powers are summarized in Table I. The linewidth of single pulse is not measured, but the envelope of several hundred pulses (which is the parameter relevant to our data) has a full width at half-maximum (FWHM) of 1–2 Å.

C. Neutral Detection

After being crossed by the pulsed laser beam in the interaction region, the remaining ions are electrostatically deflected into a shielded Faraday cup. The neutrals produced by the laser pulse impinge on the first dynode of a 15-state CuBe dynode multiplier. Owing to the large number of

TABLE I. Properties of laser dyes used in Se^- photodetachment.

Dye [a]	Tuning range (nm)	Output [b] (mJ/pulse)
Brilliant sulphaflavine [c]	518–570	1
Fluoral 7GA [c]	540–585	2
Rhodamine 6G [d]	570–620	6 [e]
Rhodamine B and Rhodamine 6G [d]	600–650 [f]	3
Cresyl violet and rhodamine 6 G [d,g]	640–700	2

[a] Typically, 2×10^{-4} M solutions in ethanol.
[b] Output with 12 J into flashlamp.
[c] Solution in equilibrium with 1-atm N_2. Cyclooctatetraene added for triplet quenching.
[d] Solution in equilibrium with 0.2-atm O_2.
[e] Laser was run at lower output level to avoid saturating the photodetachment.
[f] Output range depends on the relative concentrations of the two dyes.
[g] Rhodamine 6G is always used with cresyl violet to provide a mechanism for pump-energy transfer to the cresyl violet. By using appropriate concentrations of rhodamine 6G, rhodamine B, and cresyl violet, the laser output power can be made to peak anywhere in the range 620–680 nm.

neutrals reaching the detector in a short time, the multiplier is operated in a linear, charge-amplifying mode, rather than as a particle counter.

The multiplier signal is monitored using a matched pair of fast sample/holds (S/H). One samples the multiplier signal after a delay following the laser pulse appropriate to the neutral flight time (≈6 μsec) from the interaction region to the detector. The other samples the stripped neutral signal approximately 1 μsec before the laser-produced neutrals reach the multiplier, thus providing a neutral background correction obtained in a time short compared to the coherence time of the negative ion beam. The S/H's used have a response time of 0.3 μsec.

D. Data Acquisition

A PDP-8/L computer with ±10-V, 12-bit analog-to-digital-converter (ADC) inputs is used to control the apparatus and process the data. The ion beam current from the Faraday cup is monitored with an electrometer whose output is fed directly to the ADC. The output voltages of the two neutral-detector S/H's, along with the output voltage of a third S/H used to monitor the integrated signal from the laser photodiode, are also fed into the ADC. The triggers for the laser and the sample holds are controlled by a combination of computer-generated pulses and delay gates.

E. Data Reduction

Using a small computer to control the laser firing and read the various S/H signals, we determine an apparent relative neutral production cross section for each shot of the laser. A single datum point in one run is the average of, typically, 300 such shots. The quantity actually measured, Q_{AP}, is given in terms of our experimental parameters as

$$Q_{AP} = \frac{1}{N}\sum_{i=1}^{N} \frac{AS(i) - AB(i) - AN}{LS(i)[IS(i)]},$$

where N is the total number of laser shots for the datum point, $AS(i)$ is the signal from S/H looking at laser-produced neutrals and background-stripped neutrals for the ith laser shot, $AB(i)$ is the signal from S/H looking at stripped neutrals alone for the ith laser shot, AN is the net laser-induced electrical noise in the atom channel, $LS(i)$ is the laser signal measured by photodiode for the ith laser shot, and $IS(i)$ is the ion current measured at Faraday cup for the ith laser shot. The implicit assumption is made that the spatial overlap between the ion and laser beam is time invariant. The correction for the laser-induced electrical noise in the atom channel AN is obtained by periodically turning off the ion beam and averaging the difference between the signals from the two S/H's monitoring the neutral detector over 100 pulses of the laser. This procedure determines that portion of the difference $AS(i) - AB(i)$ which results from electrical noise generated when the laser fires. Only this channel has a detectable laser-induced electrical noise. Since, at the time of this measurement, the ion beam is off, the ion channel-zero offset is also noted and updated.

In order to correct the relative cross section for slow drifts in the system due to changes in the ion-beam–laser-beam overlap, one particular wavelength is designated as a benchmark, and the cross section at this wavelength is measured after every three data points. A linear interpolation is then performed between successive values of the benchmark cross section, and the data points are normalized to a particular value for the cross section at the benchmark. The system is considered to be functioning acceptably when the benchmark cross section varies less than 3% from run to run. The laser-induced electrical noise in the atom channel AN and the ion channel-zero offset are updated prior to each benchmark run; the laser photodiode-zero offset, prior to each shot of the laser.

Data are taken as a function of the laser grating angle. These data are converted to wavelengths by calibrating the laser with a 0.35-m monochromator whose resolution is better than 0.1 nm. The monochromator is calibrated against standard spectral lamps. A thermopile, assumed to be black over the spectral range involved, is used to determine the wavelength dependence of the photodiode response. This correction (approximately 10%/100 MeV) is applied to the data.

In order to be certain that the observed cross section is the result of an unsaturated single-photon process, the apparent cross section is measured as a function of laser power. Neutral density filters are used to vary the laser power, while ensuring a constant laser linewidth. Provided that the laser beam is not strongly focused on the ions, the cross section is constant over the available range of laser power. This apparent cross section would increase[7] with laser power for a multiphoton process; it would decrease[2] if the photodetachment were saturated.

The absolute cross section for Se^- photodetachment is estimated by measuring relative photodetachment cross sections, under identical experimental conditions, for O^- and Se^- at some fixed wavelength. These apparent relative cross sections are converted to true relative ones by making the appropriate ion-velocity correction, and determining the ratio of secondary electron

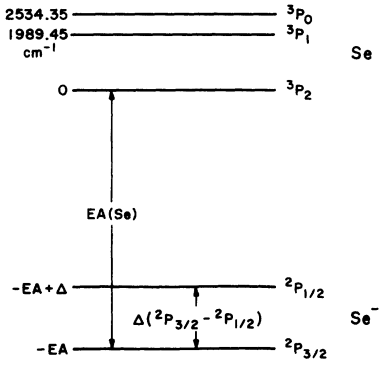

FIG. 2. Energy-level diagram for Se and Se^-.

yields for 2-keV O and Se. The Se^- absolute cross section is then found by comparison with the measured[8] absolute cross section for O^-. See Sec. III C for more details of the absolute cross-section measurement.

III. RESULTS AND DISCUSSION

A. Measurements and Extraction of Onset Energies; Determination of EA(Se) and the Se^- Spin-Orbit Splitting; Comparison with Other Determinations

From the level diagram for Se^- and Se, which is shown in Fig. 2, one expects to observe a total of six fine-structure onsets. The experimental results are shown in Fig. 3 (linear ordinate) and Fig. 4 (logarithmic ordinate). One clearly recognizes four sharp onsets, whose detailed energy dependence will be discussed later. The identification is straightforward: the strongest onsets with energy differences equal to those known from spectroscopy[9] (within ±2 cm^{-1}) correspond to transitions from $Se^-(^2P_{3/2})$ to $Se(^3P_{2,1,0})$; apparently, most of the Se^- ions in our beam are in the $^2P_{3/2}$ ground state, as expected. The onset at about 16 000 cm^{-1} is the transition $Se^-(^2P_{1/2}) \rightarrow Se(^3P_1)$. It cannot be $^2P_{1/2} \rightarrow {}^3P_0$, because then we should see an onset around 15 450 cm^{-1}, which we do not observe; it cannot be $^2P_{1/2} \rightarrow {}^3P_2$, because the cross section is nonzero below this, and there is also no indication of an onset around 18 000 cm^{-1}.

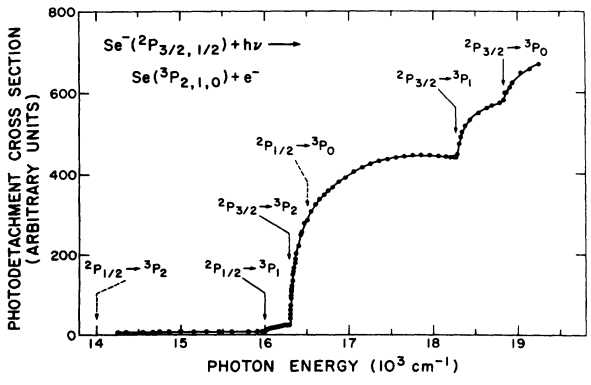

FIG. 3. Se^- photodetachment cross section in the energy range 14 000–19 000 cm^{-1}. The individual fine-structure transition thresholds are labeled. See text for details.

The range of the tunable lasers was not large enough to observe the $^2P_{1/2} \rightarrow {}^3P_2$ onset (around 14 000 cm^{-1}). The $^2P_{1/2} \rightarrow {}^3P_0$ onset is "buried" in the rising part of the first big onset (near 16 550 cm^{-1}). The electron affinity of Se, corresponding to the $Se^-(^2P_{3/2}) \rightarrow Se(^3P_2)$ threshold, was determined from plots

$$(Q/h\nu)^2 = f(h\nu),$$

where Q is the measured cross section for considered transition, and $h\nu$ is the photon energy. Dividing Q by $h\nu$ means taking out the "trivial" dependence of Q on photon energy.[8]

It was found that up to ≈5 MeV (40 cm^{-1}) above threshold these plots were straight lines; extrapolation to $Q=0$ gave the threshold energies $h\nu_{thr}$. In some cases, a comparison with calculated threshold curves was made, in which the finite energy bandwidth of the photons (≈0.3 MeV) was taken into account by convolution. One example is presented in Fig. 5; the threshold is thus determined to within 1 cm^{-1}. The result for EA(Se) is given[10] in Table II and compared with isoelectronic extrapolation (IE) data and one experimental determination[11] (surface ionization). The IE numbers[12,13] appear to be good estimates. The SI value is in good agreement with our results in this case.

The fine-structure splitting in the Se^- ion was derived from the three most precisely determined thresholds ($^2P_{1/2} \rightarrow {}^3P_1$; $^2P_{3/2} \rightarrow {}^3P_2$; $^2P_{3/2} \rightarrow {}^3P_1$) and is $\Delta E(^2P_{3/2} - {}^2P_{1/2}) = 2279 + 2\ cm^{-1} \cong 282.6 \pm 0.3$ MeV.

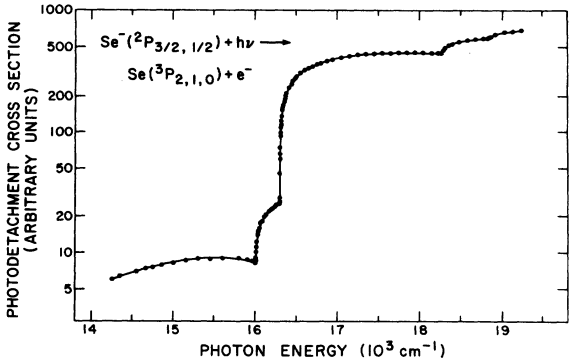

FIG. 4. Logarithmic presentation of Se^- photodetachment data.

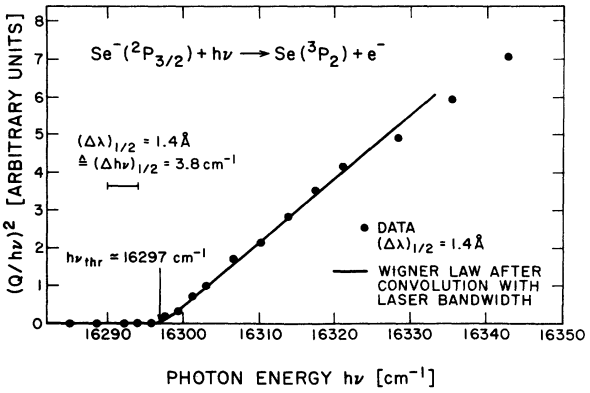

FIG. 5. High-resolution Se^- photodetachment data near the $^2P_{3/2}$-$^3P_2$ onset. The cross section in the region 16250–16290 cm^{-1} has been extrapolated into the threshold region and subtracted from the observed cross section to obtain these data. The solid curves represent the Wigner law convolved with our laser linewidth, and indicates that the threshold energy is determined to ± 2 cm^{-1}.

We have employed isoelectronic extrapolations to determine the doublet splitting in the ions O^-, S^-, Se^-, and Te^-; from comparison with the accurately known values for S^- and Se^-, we can determine how accurate extrapolation of such splittings is for negative ions. The IE procedure can then be used with some confidence to predict spin-orbit coupling constants in O^- and Te^-. One possibility is to extrapolate these splittings along the isoelectronic series by use of Sommerfeld's fine-structure formula. This procedure essentially amounts to extrapolating the screening constant, which slowly varies with atomic number.[14]

We applied a somewhat different scheme by extrapolating ratios of fine-structure intervals; these ratios appear to vary slowly with atomic number. For instance, we extrapolated the ratios (for the sulfur sequence):

$$\frac{\Delta E_{3/2-1/2}(S^-)}{\Delta E_{2-0}(S)},\ \frac{\Delta E_{3/2-1/2}(Cl)}{\Delta E_{2-0}(Cl^+)},\ \frac{\Delta E_{3/2-1/2}(Ar^+)}{\Delta E_{2-0}(Ar^{2+})},\ \ldots,$$

where $\Delta E_{3/2-1/2} = \Delta E(^2P_{3/2} - {}^2P_{1/2})$, $\Delta E_{2-0} = \Delta E(^3P_2 - {}^3P_0)$, and $\Delta E_{3/2-1/2}$ of the negative ion is regarded as unknown. This procedure has the advantage that the existing knowledge on the fine-structure spacing of the neutral species A is included in extrapolating to the splitting for A^-. Figure 6 shows the corresponding plots for the cases of the O and S sequences. For the Se and Te sequences, less spectroscopic information exists, and the values obtained are less accurate.

As seen from Table III, the extrapolated values for S^- and Se^- agree very well with the experimental results. There is a striking discrepancy, however, in the case of O^-, for which Berry *et al.*[15] (in a radiative attachment experiment) found a value some 50% higher than the extrapolated value. Branscomb *et al.*[16] obtained 230 cm^{-1} by isoelectronic extrapolation of the $\Delta E_{3/2-1/2}$ intervals to that for O^-, employing a polynominal extrapolation technique. We do not understand the discrepancy with respect to our result. We have also extrapolated the O^- splitting by use of Sommerfeld's formula and obtained 182 ± 5 cm^{-1}, in excellent agreement with the result extracted from the plot in Fig. 6. Since our extrapolation method was tested for S^- and Se^-, where it gives very good results, we are confident that the true value for the spin-orbit splitting in O^- is within the range 181 ± 4 cm^{-1}.

In this context we would like to note that the value for the electron affinity (EA) of O, determined by Berry *et al.*[15] [(1.478 ± 0.002) eV], is also distinctly higher than the photodetachment value of Branscomb *et al.*[8,16] [(1.465 ± 0.005) eV]. Tunable dye-laser experiments done in this laboratory on the $O^-(^2P) \rightarrow O(^1D)$ photodetachment onset indicate[2] that the value of Branscomb *et al.* is probably correct within its error limits. We find EA(O) $= 1.462^{+0.003}_{-0.007}$ eV. Finally, we note that Chupka[17] determined EA(O) from high-resolution pair-production photoionization studies of O_2 around 720 Å. He finds EA(O) is essentially in agreement with our result.

TABLE II. Electron affinity of $Se(^3P_2)$.

	This work	IE horizontal analysis [a]	IE vertical analysis [b]	Experimental surface ionization [c]
EA(Se)	2.0206 ± 0.0003 eV 16297 ± 2 cm^{-1}	2.12 ± 0.2 eV	2.11 eV	~2 eV

Conversion: 1 eV ≅ 8065.466 cm^{-1}.
[a] Reference 12.
[b] Reference 13.
[c] Reference 11.

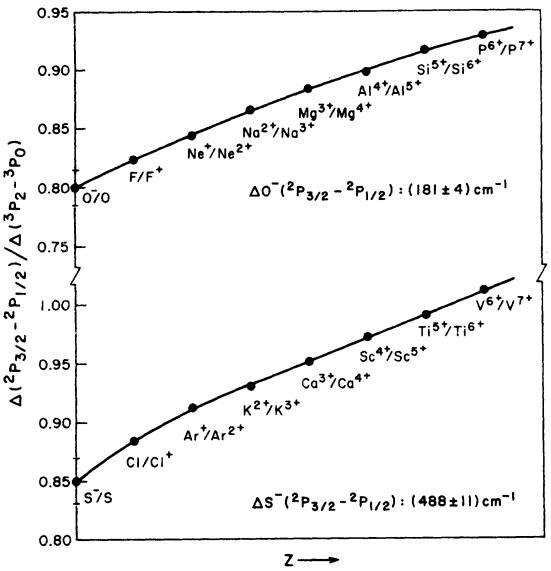

FIG. 6. Isoelectronic extrapolations of fine-structure intervals in the S and O isoelectronic sequences. See text for details of the procedure employed.

B. Transition Strengths for Various Fine-Structure Onsets in Se^- Photodetachment

We now discuss the transition strengths of the various fine-structure transitions $Se^-(^2P_{3/2,\,1/2}) \rightarrow Se(^3P_{2,\,1,\,0})$. The transition strength S_j shall be defined according to the convention employed by Rau and Fano,[18] i.e.,

$$\sigma_j = cS_j h\nu k[1 + \text{correction terms}],$$

where σ_j is a cross section for transition j, and c is a constant, which is the same for all j. The S_j's are experimentally derived from threshold plots (Figs. 7–9)

$$(\sigma_j/h\nu) = cS_j k.$$

Numbers obtained in this way appear to have good individual accuracy; larger uncertainties are introduced, however, as a result of the necessity to splice together data that were taken with different dyes, the wavelength region of overlap being 100 Å or less. Thus the uncertainty of the $^2P_{3/2} \rightarrow {}^3P_{1,0}$ strengths relative to the $^2P_{3/2} \rightarrow {}^3P_2$ strength is larger than the one determined from the respective threshold plots alone.

TABLE III. Spin-orbit splittings in Column VI negative ions in cm^{-1}.

	Experimental	IE other work	IE this work
O^-	285 ± 15 [a]	230 [b]	181 ± 4
S^-	482 ± 2 [c]	•••	488 ± 11
Se^-	2279 ± 2 [d]	2322 [e]	2290 ± 50
Te^-	•••	5082 [e]	5000 ± 150

[a] Reference 15.
[b] Reference 16.
[c] Reference 1.
[d] This work.
[e] Reference 12.

The results are summarized in Table IV; predictions obtained from different theoretical models are given for comparison. The factor τ accounts for the fact that the relative population of the negative-ion fine-structure states in the experiment is not given by $N(\frac{1}{2})/N(\frac{3}{2}) = \frac{1}{2}$, as assumed in the calculation of the theoretical numbers. Comparing experiment and theory, we obtain a value for τ which may be interpreted in terms of an effective ion-source temperature via the relation

$$\tau = e^{-\Delta E_{3/2-1/2}/kT},$$

where $\Delta E_{3/2-1/2}$ is the energy separation between the $Se^-(^2P_{3/2,\,1/2})$ states. We find $\tau = 0.145$ to be a reasonable choice (corresponding to $T = 1700\,^\circ K$). It should be noted that the relative population of the $Se^-(^2P_{1/2,\,3/2})$ levels was found to vary by ±40% with changes in the ion-source discharge parameters.

The statistical model ignores the outgoing elec-

TABLE IV. Transition strengths for various fine-structure onsets in Se^- photodetachment. [$\tau \equiv e^{-[2279/kT(cm^{-1})]}$. $\tau = 0.14_5$ gives good fit to our data. Numbers in ( ) were calculated using $\tau = 0.14_5$.]

Se^-	Se	This work	Rau and Fano	Complex model	Statistical
	$^3P_2$	[100]	[100]	[100]	[100]
$^2P_{3/2}$	$^3P_1$	33 ± 3	36	120	60
	$^3P_0$	15 ± 4	8	20	20
	$^3P_2$	2.5 ± 0.5	20τ(2.9)	20τ(2.9)	50τ(7.8)
$^2P_{1/2}$	$^3P_1$	5.5 ± 0.5	36τ(5.2)	60τ(8.7)	30τ(4.4)
	$^3P_0$	•••	16τ(2.3)	40τ(5.8)	10τ(1.5)

tron, assuming that the strengths of all transitions are inherently the same, except for multiplication by the level degeneracy $(2J+1)$ in the final state. The statistical model fails to provide a good prediction of the transition strengths, as is particularly apparent in the $^2P_{1/2} \rightarrow {}^3P_{2,1,0}$ branch. This model simply assumes that the strengths are proportional to the products of the statistical weights of the fine-structure levels involved in the various transitions.

The complex model[1] for S^- detachment is based on the idea that near threshold one should view the final state as a comples $(e+S)$ in LS coupling. The transition strengths are determined by calculating the optical transition strengths going from the LS-coupled negative-ion state to the intermediate LS-coupled state, and further by assuming that each of these LS-intermediate states splits evenly into the alternative fine-structure levels of S. This model provides rather good agreement with experiment for the $^2P_{1/2} \rightarrow {}^3P_{2,1,0}$ transitions, but the agreement is not as good for the $^2P_{3/2} \rightarrow {}^3P_{2,1,0}$ branch.

In a recent paper, Rau and Fano[18] have extended the idea of the complex model by considering in detail the dissociation of the intermediate complex into the various exit fine-structure levels. They used the method of "frame transformation" for projecting the LS-intermediate states onto the final jj-coupled states in a general treatment for negative ions of $p^5(^2P_{3/2,1/2})$ configuration. As was observed in the case of S^-, the Rau and Fano model for the Se^- fine-structure transition strengths provides by far the best agreement with our Se^- data. A virtue of their treatment is that their numbers for the various transition strengths are relatively insensitive to the physical parameters which describe the electron-atom interaction in the exit channel. Rau and Fano cast all of these interactions into the two scattering lengths a_d and a_q (doublet and quartet scattering lengths in this case). Their expressions for the energy dependence of the cross sections depend basically on a_d and a_q, as do the transition strengths, but an inspection of their formula shows that the variation of the latter with a_d and a_q is small. This is particularly true when the fine-structure splittings are small, as for instance in the case of oxygen.

A deficiency of their model is the neglect of long-range forces (such as e^--induced dipole, etc.). It is not obvious to us in which way their predictions of the transition strength would be changed by incorporating long-range forces into the model; we believe, however, that they would vary little.

Another interesting question is how the gradual change from LS coupling to jj coupling for the initial and intermediate state, as when going from O^- to Te^- within the sixth column of the Periodic Table, would influence the predictions made within a modified Rau-Fano model.

C. Determination of Absolute Cross Section for $Se^-(^2P_{3/2})$ Detachment

During the course of the experiments we also determined the absolute cross section for $Se^-(^2P_{3/2})$ photodetachment. To obtain this result, we compared the detachment signals for O^- and Se^- at a number of photon energies in the range 17 000–18 200 cm^{-1}. The cross section for O^- detachment is known to be constant in this energy range and has a value[16] of $\sigma = 6.3 \times 10^{-18}$ cm^2. The Se^- cross section is obtained from

$$\sigma(Se^-) = \frac{Q_{AP}(Se^-)}{Q_{AP}(O^-)} \frac{\gamma(O)}{\gamma(Se)} \frac{v(Se^-)}{v(O^-)} \sigma(O^-),$$

where Q_{AP} is an apparent cross section (proportional to signals observed, see Sec. II); γ is the yield for ejection of secondary electrons at the cathode of the multiplier, which detects neutrals created in the detachment process; v is the velocity of ions in the detachment chamber; and σ is the absolute cross section. Care was taken that there was no saturation[2] of detachment. By using different laser beam configurations—focused, unfocused, telescope expanded—we tried to test the question of possible differences in overlap of the laser beam with the O^- and Se^- ion beams; the results of these measurements were satisfactory in that no appreciable differences ($\lesssim 5\%$) in the relative apparent cross sections were found. The largest error appears to be introduced by the ratio $\gamma(O)/\gamma(Se)$. The reproducibility of the measured ratio $\gamma(O^-)/\gamma(Se^-)(\approx 1.8)$ on different days was 10–15%. Evidence from other experiments[19] leads us to conclude that $\gamma(O)/\gamma(Se) \approx \gamma(O^-)/\gamma(Se^-)$ at 2 keV energy to within about 10–20%.

We estimate $\sigma(Se^-)$ to be accurate to about ±30%. The result for the $Se^-(^2P_{3/2}) \rightarrow Se(^3P_2)$ cross section at 18 000 cm^{-1} is

$$\sigma[Se^-(^2P_{3/2}) \rightarrow Se(^3P_2)] = (7.5 \pm 2) \times 10^{-18}\ cm^2.$$

A minor correction has been made by subtracting out the signal at 18 000 cm^{-1} from $Se^-(^2P_{1/2}) \rightarrow Se(^3P_{2,1,0})$ transitions; the uncertainty in this correction contributes little to the 30% error mentioned. The analysis was based on the estimate for the relative population of the $^2P_{1/2}$ and $^2P_{3/2}$ states of Se^- in the ion beam, given in Table IV.

D. Theory of Threshold Behavior of Photodetachment Cross Sections and Comparison with Experiment

In this section we will discuss in more detail the threshold behavior of the photodetachment

cross section and what may be learned from a precise experimental determination of it. As mentioned in the Introduction, Wigner,[3] in his general paper on the threshold energy dependence of processes in which pairs of particles are formed, gives the leading term as

$$\sigma \propto k^{2L+1} \tag{2a}$$

for the case in which the final-state interaction (other than the centrifugal potential) falls off faster than $1/r^2$. In photodetachment, k is very close to the electron momentum and L is its orbital angular momentum with respect to the atom. If one calculates the photodetachment cross section using standard perturbation theory, as is done by Branscomb *et al.*,[16] one obtains

$$\sigma = ch\nu k|M_{if}|^2, \tag{3}$$

where $h\nu$ is the photon energy, c is a constant, and M_{if} is the dipole matrix element for the photodetachment transition.

For short-range potentials (such as square-well or Yukawa-type potentials) one can show that

$$|M_{if}|^2 = k^{2L}(b_1 + b_2k^2 + \cdots),$$

where b_1, b_2, ... are constants. Since $h\nu = E_{\text{thr}} + E_{\text{el}} = d_1 + d_2k^2$ (E_{thr} is the threshold energy for the transition under investigation; E_{el} is the electron kinetic energy in final state; d_1, d_2 are constants), Wigner's law can be written

$$\sigma = ck^{2L+1}[1 + O(k^2)] \tag{4}$$

for short-range potentials in the exit channel. The quantity $O(k^2)$ contains terms proportional to k^2 and higher-order terms.

O'Malley[4] investigated the influence of long-range potentials on the photodetachment cross section near threshold. For $V(r) \propto 1/r^2$ [as in the case of an electron-dipole interaction, e.g., $H(n=2) + e^-$], deviations from the basic Wigner law (2) are predicted; this result is to be expected, since Wigner's basic assumption on the nature of the long-range potentials does not hold in this case. O'Malley[4] has also investigated the effect of the electron-induced dipole interaction,

$$V(r) = -(\alpha e^2/2r^4), \tag{5}$$

where α is the static dipole polarizability of final-state atom A and e is electron charge. Wigner derived the following modification[20] to Eq. (4):

$$\sigma = ck^{2L+1}\left(1 - \frac{4\alpha k^2 \ln k}{a_0(2L+3)(2L+1)(2L-1)} + O(k^2)\right), \tag{6}$$

where a_0 is the Bohr radius and α, k are in atomic units.

It is interesting to note that this new correction term is negative for $L=0$, whereas it is positive for $L>0$ (only $k \ll 1$ is considered). This sign change may be qualitatively understood by noting that the $1/r^4$ potential, which is always attractive, decreases the centrifugal barrier for $L>0$, which results in an increased cross section, while for $L=0$ the leaving electron is "reattracted" to the atom, leading to a decrease in cross section.

Unfortunately, Eq. (6) contains terms of order k^2, whose coefficients are unknown, so that a comparison with experiment may not be particularly exciting. The k^2 terms have to be included in the expression for σ. (The $k^2 \ln k$ term was derived from an expression $k^2 \ln c_1 k$ and, in addition, other terms of order k^2 appear; see also footnote 10 in Ref. 4.) One might think that the appearance of a $k^2 \ln k$ term can be distinguished from k^2 terms in a fitting procedure, when compared with accurate experimental cross sections. It turns out, however, that over the region of k values ($k_{\min} \leq k \leq k_{\max}$), where (i) Eq. (6) is applicable ($k \leq k_{\max}$) *and* (ii) the correction term is large enough ($k \geq k_{\min}$) to be significant, the $\ln k$ factor varies too little to get independent numbers for the coefficients of the $k^2 \ln k$ and the k^2 terms in a least-squares fit to the experimental data.

This fact does not necessarily mean that one is not able to provide some evidence for the existence of the O'Malley correction term, since it may be that a theoretical fit with Eq. (6) gives distinctly better agreement with experiment than a fit with Eq. (4), which omits the $k^2 \ln k$ term.

The idea in O'Malley's treatment,[4] which is based on the modified effective-range theory (MERT) developed by O'Malley, Spruch, and Rosenberg[21] is that the *major* energy dependence of the correction terms in Eq. (6) originates from the energy dependence of the normalization factor to the radial wave function, provided that the latter is chosen to be energy independent at small distances (where the matrix element is evaluated).

To be more specific, we note that a wave function with the usual asymptotic form

$$u_L(r) \sim (1/kr)\sin(kr - \tfrac{1}{2}L\pi + \eta_L) \tag{7}$$

is energy dependent at small r, and the matrix element M_L calculated using $u_L(r)$ is $\propto k^L$. O'Malley considered the (exact) solutions to the Schrödinger equation for a $1/r^4$ potential (modified Mathieu functions) and chose them to be energy independent at small r. These solutions, $\tilde{u}_L(r)$, have the asymptotic form

$$\tilde{u}_L(r) \sim [N_L(k)/kr]\sin(kr - \tfrac{1}{2}L\pi + \eta_L), \tag{8}$$

where $N_L(k)$ is an energy-dependent renormalization factor. Equation (3) for the cross section then

becomes

$$\sigma_L = \text{const}\left(k\frac{1}{|N_L(k)|^2}|\tilde{M}_L|^2\right), \quad (9)$$

where $|\tilde{M}_L|^2 = \text{const} + O(k^2)$ for all L owing to the energy independence of $\tilde{u}_L(r)$ at small r ($\tilde{M}_L$ is evaluated using $\tilde{u}_L$). O'Malley[4] derived $N_L(k)$ within the frame of the MERT and arrived at Eq. (6).

One can go beyond Eq. (6), if one assumes that the terms of $O(k^2)$ which come from $|\tilde{M}_L|^2$ can be neglected in comparison with those originating from $N_L(k)$. If the expansion for $N_L(k)$ is carried through to include explicitly the terms of order k^2 and k^3 in MERT, as outlined in the Appendix, one obtains the following expression for the cross section, for the simplest case $L=0$:

$$\sigma_0 = (\text{const})h\nu k[1 + \tfrac{4}{3}\beta^2k^2\ln 1.23\beta k + Ak^2(r_{p_0} + \tfrac{2}{3}\pi\beta - A) - \tfrac{4}{3}\pi\beta^2Ak^3], \quad (10)$$

where $\beta^2 = \alpha/a_0$, A is the scattering length, and r_{p_0} is the modified effective range.

We see that all the parameters that are used to describe low-energy electron-atom scattering appear in this formula: α, A, r_{p_0}. This has to do with the fact that photodetachment can be viewed as "half an elastic scattering process," and near threshold, modified effective range theory may be applied. Equation (10) is valid only if the following conditions are met: (i) The energy dependence of $|\tilde{M}_L|^2$ is small compared to the one given in large parentheses in (9), (ii) the atom A is in a state with $J=0$, and (iii) the expansion parameter $\beta k \ll 1$.[22] If (ii) does not hold ($J>0$), one has to deal with two scattering lengths. Moreover, for $J \geq 1$, the atom A will in general have a permanent quadrupole moment, which complicates the long-range potential appreciably.

O'Malley[4] has investigated the effect of an electron-permanent quadrupole potential with angular dependence $P_2(\cos\theta)$ on the photodetachment cross section. A correction term proportional to k, which would be present for a spherically symmetrical $1/r^3$ potential, was found to vanish in the angular average. Instead of Eq. (6), O'Malley found for $L=0$:

$$\sigma_0 = (\text{const})k\left\{1 + \left[\frac{19}{210}\left(\frac{Q_{av}}{ea_0}\right)^2 + \frac{4}{3}\alpha_{av}\right]k^2\ln k + O(k^2)\right\}, \quad (11)$$

where

$$\left(\frac{Q_{av}}{ea_0}\right)^2 = \frac{(J+1)(2J+3)}{5J(2J-1)}\left(\frac{Q}{ea_0}\right)^2, \quad (12)$$

with[23]

$$Q = 2e\int d\tau \sum_{j=1}^{Z_A} r_j^2 P_2(\cos\theta_j)|\psi_0|^2_{M=J}, \quad (13)$$

which is essentially the expectation value of the quadrupole operator for the state $M=J$. The quantity α_{av} is the spherically symmetric component of the polarizability.

The transition most carefully studied experimentally, $Se^-(^2P_{3/2}) - Se(^3P_2)$, shows deviations from the leading Wigner term which become clearly visible around 4–5 meV above threshold. Figure 7 shows a plot of the cross section, divided by the photon energy, versus electron momentum k in the range $0 \leq k \lesssim 0.1$ a.u. Theoretically, a final $^3P_2$ state is a rather unfavorable, complicated case. A fit with Eq. (11), which for this case ($J=2$) reads

$$\frac{\sigma_0}{h\nu} = c_1k\left\{1 + \left[\frac{19}{300}\left(\frac{Q}{ea_0}\right)^2 + \frac{4}{3}\alpha_{av}\right]k^2\ln k + c_2k^2\right\}, \quad (14)$$

would yield—besides a value for c_1 from the absolute cross-section measurement—a number for c_2, if Q and α_{av} were known. α_{av} has been recently determined in a Hartree-Fock calculation by Thorhallsson *et al.*,[24] who give the value $\alpha(\text{Se}) = 30.4a_0^3$. No value for $Q[\text{Se}(^3P_2)]$ has been reported to our knowledge. Since the coefficient of the quadrupole term is small, it may be justifiable to neglect it, compared to the polarizability term.

We have also tried a fit with Eq. (10), although we are aware that it does not describe a $J=2$ case. One may visualize the quantity A as being an effective scattering length averaged over the doublet and quartet contributions, a_d and a_q. We set $\alpha = 30.4a_0^3$ and $r_{p_0} = 0$ and obtain[25] $A \approx -6a_0$ from a fit to our data. This result is physically reasonable, since it indicates that one should observe a Ramsauer minimum in low-energy e^--Se scattering, as expected for an atom of such a large polarizability.

We have not tried fits with expressions other

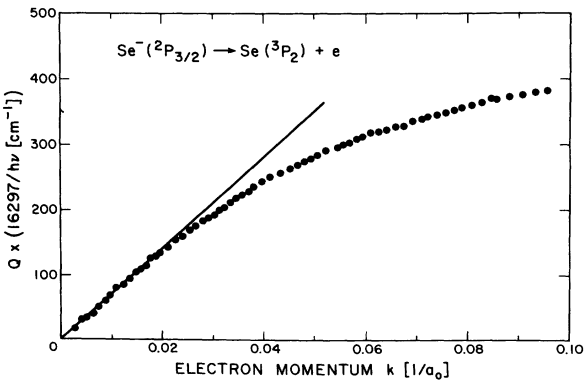

FIG. 7. $Se^-\ ^2P_{3/2} - Se\ ^3P_2$ partial photodetachment cross section plotted as a function of electron momentum. The straight line is the Wigner threshold law, which is seen to be valid for only the first 5 MeV (0.02 a.u.) above threshold.

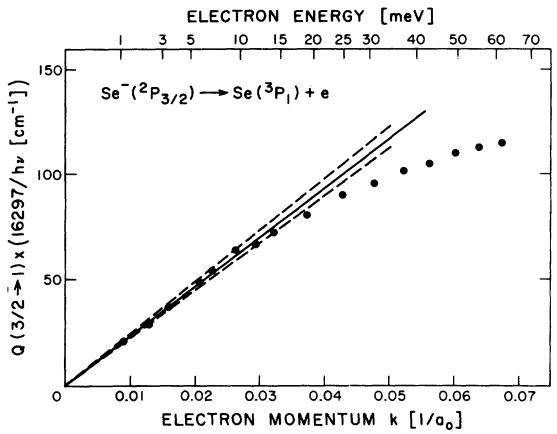

FIG. 8. $Se^- {}^2P_{3/2}$ - $Se\ {}^3P_1$ partial photodetachment cross section. The dashed lines indicate the uncertainty in the Wigner law fit.

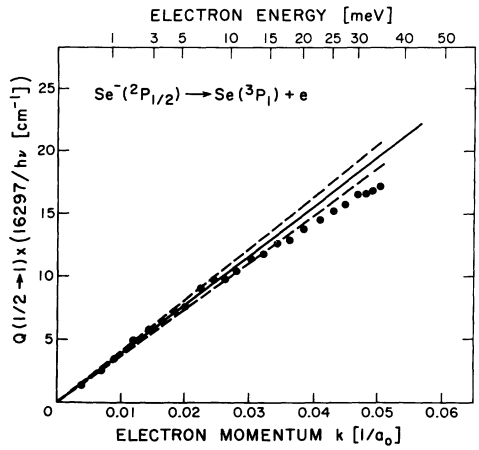

FIG. 9. $Se^- {}^2P_{1/2}$ - $Se\ {}^3P_1$ partial photodetachment cross section. Note that the departures from the Wigner law are less pronounced here than in the $^3P_2$ case of Fig. 7.

than those of the basic form (6), because we feel there is no physical justification for expressions such as $\sigma = c_1 k^b$ or $\sigma = c_1 k(1+dk)$ which were used by Steiner[26] in order to fit his low-resolution S^- photodetachment data.

Figures 8 and 9 present the plots corresponding to that in Fig. 7 for the $\frac{3}{2} \rightarrow 2$ onset for the two transitions $^2P_{3/2} \rightarrow {}^3P_1$ and $^2P_{1/2} \rightarrow {}^3P_1$. Since the two final states are identical, one expects the energy dependence to be the same, as is indeed the case within experimental errors. It appears that for these two onsets the deviations from Wigner's law set in somewhat later (around $k \approx 0.03$) than for the $^2P_{3/2} \rightarrow {}^3P_2$ onset. Since the long-range parameters are different for the $({}^3P_2 + e^-)$ and $({}^3P_1 + e^-)$ final states, one expects to observe some differences. Which of the different parameters is primarily responsible for the observed change (which is not large), we cannot conclude from our data, because neither the polarizability nor the quadrupole moment is known for the $^3P_2$, $^3P_1$ states, nor are the doublet and quartet scattering lengths associated with either $^3P_2$ or $^3P_1$.

IV. CONCLUSIONS

A pulsed tunable dye laser has been used to study photodetachment of Se^- ions in a crossed-beam experiment. A detailed description of the apparatus and techniques has been presented. The threshold behavior of the photodetachment cross section is compatible with the Wigner threshold law[3] over about 5 meV. Four of the six fine-structure transitions are observed and identified, with the result that EA(Se) = (2.0206 ± 0.0003) eV and the spin-orbit splitting between the $^2P_{3/2}$ and $^2P_{1/2}$ states in Se^- is (2279 ± 2) cm^{-1}. The transition strengths for the various fine-structure transitions have been determined and found to be in very good agreement with the predictions[18] by Rau and Fano. Since the experimental data indicate large departures from the Wigner threshold law close to threshold, we have attempted to extend the treatment of O'Malley,[4] in the frame of modified effective-range theory, in an attempt to explain the cross-section behavior above threshold. Finally, the absolute cross section for $Se^-(^2P_{3/2})$ photodetachment 1700 cm^{-1} above threshold is found to be $(7.5 \pm 2) \times 10^{-18}$ cm^2.

ACKNOWLEDGMENTS

We have benefited greatly from stimulating conversations with Dr. D. Norcross and instructive correspondence with Professor T. F. O'Malley.

APPENDIX

Equation (10) is an extension of O'Malley's[4] result, Eq. (6), for $L = 0$. The derivation is based on formulas in the MERT paper by O'Malley, Spruch, and Rosenberg.[21] Therein two independent solutions to the Schrödinger equation with potential $V(r) = -(\beta^2 e^2/2r^4)$ $(\beta^2 = \alpha/a_0)$ are chosen in such a way that they are energy independent at small r, and for large r they behave as

$$v_{ps} \sim \frac{(-1)^L m}{(\beta k)^{1/2} \cos 2\delta}\left[\left(\cos^2\delta - \frac{\sin^2\delta}{m^2}\right)\cos\left(kr - \frac{L\pi}{2}\right) + \sin\delta\cos\delta\left(\frac{1}{m^2} - 1\right)\sin\left(kr - \frac{L\pi}{2}\right)\right],$$

$$v_{pc} \sim \frac{(-1)^L m}{(\beta k)^{1/2} \cos 2\delta}\left[\sin\delta\cos\delta\left(1 - \frac{1}{m^2}\right)\cos\left(kr - \frac{L\pi}{2}\right) + \left(\frac{\cos^2\delta}{m^2} - \sin^2\delta\right)\sin\left(kr - \frac{L\pi}{2}\right)\right]. \quad \text{(A1)}$$

Here v_{ps} and v_{pc} are functions, which represent $r\times$ (actual radial function); they are modified Mathieu functions with

$$m \equiv \frac{M_\nu^{(1)}(0)}{M_{-\nu}^{(1)}(0)} = \left(\frac{\beta k}{4}\right)^\nu \frac{\Gamma(1-\nu)}{\Gamma(1+\nu)} \times\left(1 - \frac{\nu}{4(1-\nu^2)^2}\beta^2k^2 + O(k^4)\right), \quad \text{(A2)}$$

where ν is the characteristic index of modified Mathieu functions,

$$\nu = L + \tfrac{1}{2} - \frac{2\beta^2k^2}{(2L+3)(2L+1)(2L-1)} + O(k^4). \quad \text{(A3)}$$

Further, we find

$$\delta \equiv \tfrac{1}{2}\pi(\nu - L - \tfrac{1}{2}). \quad \text{(A4)}$$

If the asymptotic form of the wave function of an elastically scattered electron is written as $v_p = v_{ps} + Bv_{pc}$ and one inserts (A1), one obtains, at large r,

$$v_p = \frac{(-1)^L C}{(\beta k)^{1/2} m(1-\tan^2\delta)} \times\left[\sin\left(kr - \frac{L\pi}{2}\right) + \frac{S}{C}\cos\left(kr - \frac{L\pi}{2}\right)\right], \quad \text{(A5)}$$

with

$$S = m^2 - \tan^2\delta + B\tan\delta(m^2 - 1), \quad \text{(A6)}$$

$$C = (1-m^2)\tan\delta + B(1 - m^2\tan^2\delta). \quad \text{(A7)}$$

The phase shift is thus given by

$$\tan\eta_L = S/C \quad \text{(A8)}$$

and is closely connected with B. In MERT, B is given by

$$B/\beta = -1/A + \tfrac{1}{2}r_{p_0}k^2 + O(k^4), \quad \text{(A9)}$$

when A is the scattering length;

$$\lim(\tan\eta_0/k) \text{ as } k \to 0 \equiv -1/A = \beta/B_0 \quad \text{(A10)}$$

and

$$r_{p_0} \equiv 2\int_0^\infty (v_{p_0}^2 - u_0^2)\,dr, \quad \text{(A11)}$$

where v_{p_0} is the solution of the Schrödinger equation with $V(r) = -(\alpha e^2/2r^4)$ for all r, and where u_0 is the solution of the Schrödinger equation with true $V(r)$ (both v_{p_0} and u_0 are taken in the $k \to 0$ limit).

We compare (A5) with the wave function of the photodetached electron $\bar{v}$ in order to determine $N_L(k)$ in terms of β, A, and v_{p_0}.

At large r:

$$\bar{v} = [N_L(k)/k]\sin(kr - \tfrac{1}{2}L\pi + \bar{\eta}_L) = [N_L(k)/k]\cos\bar{\eta}_L[\sin(kr - \tfrac{1}{2}L\pi) + \tan\bar{\eta}_L\cos(kr - \tfrac{1}{2}L\pi)]. \quad \text{(A12)}$$

The connection of photodetachment with elastic scattering lies in the assumption that the phase shifts η_L and $\bar{\eta}_L$ are equal which, we think, is a very good approximation. Thereby one gets, comparing (A5) and (A12),

$$N_L(k) = \frac{(-1)^L kC}{(\beta k)^{1/2} m(1-\tan^2\delta)\cos\eta_L} = \frac{(-1)^L k(S^2+C^2)^{1/2}}{(\beta k)^{1/2} m(1-\tan^2\delta)},$$

since

$$\cos\eta_L = \frac{C}{(S^2+C^2)^{1/2}};$$

and since

$$\sigma_L = (\text{const})kh\nu[|\bar{M}_L|^2/|N_L(k)|^2],$$

we get

$$\sigma_L = (\text{const})h\nu[m^2/(S^2+C^2)]|\bar{M}_L|^2,$$

where $(1-\tan^2\delta)^2 \approx 1$, because terms of $O(k^4)$ are neglected. If one works out the expansions for m^2 and S^2+C^2 in terms of β, A, and r_{p_0}, using (A2), (A3), (A4), and (A9), and if one assumes the variation of $|\bar{M}_L|^2$ with k to be negligible as compared to the one arising from $|N_L(k)|^2$, one obtains for $L=0$:

$$\sigma_0(k) = c_1 h\nu k[1 + \tfrac{4}{3}\beta^2k^2\ln 1.23\beta k + (Ar_{p_0} - A^2 + \tfrac{2}{3}\pi\beta A)k^2 - \tfrac{4}{3}\pi\beta^2Ak^3],$$

which is the result given in Eq. (10).

---

*Research supported by the Advanced Research Projects Agency of the Department of Defense and monitored by the U. S. Army Research Office-Durham under Contract No. DAHCO4-72-C-0047.

†On leave from Fakultät für Physik, Universität Freiburg, Freiburg Br, Germany; support by the Deutsche Forschungsgemeinschaft is gratefully acknowledged.

‡Alfred P. Sloan Foundation Fellow.

[1]W. C. Lineberger and B. W. Woodward, Phys. Rev. Lett. **25**, 424 (1970).

[2]H. Hotop and W. C. Lineberger, J. Chem. Phys. **58**, 2379 (1973); H. Hotop, R. A. Bennett, and W. C. Lineberger, J. Chem. Phys. **58**, 2373 (1973).

[3]E. P. Wigner, Phys. Rev. **73**, 1002 (1948).

[4]T. F. O'Malley, Phys. Rev. **137**, A1668 (1965).

[5]K. C. Smyth and J. I. Brauman, J. Chem. Phys. **56**, 5993 (1972).

[6]D. A. Jennings and D. L. Baldwin, Natl. Bur. Std. Tech. Note 603 (U. S. GPO, Washington, D. C., 1971).

[7]W. C. Lineberger and T. A. Patterson, Chem. Phys. Lett.

13, 40 (1972).
[8]L. M. Branscomb, S. J. Smith, and G. Tisone, J. Chem. Phys 43, 2906 (1965).
[9]C. E. Moore, *Atomic Energy Levels*, Natl. Bur. Std. Circ. No 467 (U. S. GPO, Washington, D. C., 1949).
[10]The preliminary number for EA(Se) given earlier [Bull. Am. Phys. Soc. 17, 150 (1972)] was lower by 0.5 meV as a result of using a wrong conversion factor from cm^{-1} to eV; the actual earlier result in cm^{-1} agrees with the present one to within 1 cm^{-1}. The $^2P_{3/2} \rightarrow {}^2P_{1/2}$ splitting was given in cm^{-1} and was therefore not affected.
[11]I. N. Bakulina and N. I. Ionov, Zh. Fiz. Khim. 33, 2069 (1959).
[12]R. J. Zollweg, J. Chem. Phys. 50, 4251 (1969).
[13]P. Politzer, Trans. Faraday Soc. 64, 2241 (1968).
[14]B. Edlén, in *Handbuch der Physik*, edited by S. Flügge (Springer, Berlin, 1956), Vol. 27, p. 165.
[15]R. S. Berry, J. C. Mackie, R. L. Taylor, and R. Lynch, J. Chem. Phys. 43, 3067 (1965).
[16]L. M. Branscomb, D. S. Burch, S. J. Smith, and S. Geltman, Phys. Rev. 111, 504 (1958).
[17]W. A. Chupka (private communication).
[18]A. R. P. Rau and U. Fano, Phys. Rev. A 4, 1751 (1971).
[19]M. D. Scheer, J. Res. Natl. Bur. Stand. (U.S.) A 74, 37 (1970).
[20]The sign of the new correction term was given incorrectly in Ref. 4; see also O. Hinckelmann and L. Spruch, Phys. Rev. A 3, 642 (1971).
[21]T. F. O'Malley, L. Spruch, and L. Rosenberg, J. Math. Phys. 2, 491 (1961); T. F. O'Malley, Phys. Rev. 130, 1020 (1963); see also B. R. Levy and J. B. Keller, J. Math. Phys. 4, 54 (1963).
[22]O'Malley (Ref. 21) states a less severe condition: $\beta^2 k^2 \ll 1$. One should keep in mind that MERT is concerned here with expansions around zero energy ($k \rightarrow 0$).
[23]T. F. O'Malley, Phys. Rev. 134, A1188 (1964).
[24]J. Thorhallsson, C. Fisk, and S. Fraga, Theor. Chim. Acta 10, 388 (1968).
[25]An inspection of the quality of the fit for various (A, r_{p_0}) combinations appears to justify $r_{p_0} = 0$ or very close to zero. We fitted our data over different ranges ($k_{max} = 0.035$, 0.05, 0.075) and found A to be essentially stable (-6 ± 0.2).
[26]B. Steiner, in *Sixth International Conference on the Physics of Electronic and Atomic Collisions: Abstract of Papers* (MIT Press, Cambridge, Mass., 1969), p. 535.

PHYSICAL REVIEW A VOLUME 8, NUMBER 2 AUGUST 1973

Measurement and Calculation of the Stark-Broadening Parameters for the Resonance Lines of Singly Ionized Beryllium*

A. Sanchez,† M. Blaha, and Walter W. Jones
Department of Physics and Astronomy, University of Maryland, College Park, Maryland 20742
(Received 18 April 1973)

The electron-impact-broadened profile of the resonance doublet of singly ionized beryllium ($2s$-$2p$, $\lambda = 3130.4$ and 3131.1 Å) has been measured using an electromagnetically driven shock tube and a rapid-scanning Fabry-Perot spectrometer. For the conditions $N_e = 10^{17}$ cm^{-3} and $T = 19\,000$°K, we found the Lorentz half-width of each line in the doublet to be 0.035 Å ± 15%. For comparison with theory, we did both a quantum-mechanical (using the close-coupling method) and a semiclassical calculation, obtaining the values 0.015 and 0.042 Å, respectively. Possible reasons for the discrepancy are discussed.

I. INTRODUCTION

From previous measurements[1] on calcium and magnesium, we have concluded that although the agreement between measured and calculated Stark widths was good, there was still a significant discrepancy, particularly with the results obtained using the quantum-mechanical (close-coupling)[2] theory. In a more recent paper[3] it was shown that the semiclassical theory agrees quite well with measurements of Stark parameters of singly ionized atoms so that we now wanted to find a definitive test for the quantum theory. To this end, we chose a first ion which was nonhydrogenic, namely, singly ionized beryllium (lithiumlike). Its resonance doublet can be measured and provides a simple atomic system with which to work (one electron outside of a closed shell) so that we might determine whether or not there is a fundamental problem with the application of current quantum-mechanical theories to broadening of spectral lines.

Our notation is that i,f refer to the initial and final energy levels, respectively, and that i',f' are nearby states which perturb (in the perturbation-theory sense) the i,f levels. We also use the usual definition of shift and width, namely, the shift is the distance of the profile maxima from the position of the unperturbed lines ($N_e \rightarrow 0$) which should be the same (to the accuracy of our experiment) for both lines in the doublet, and the width is one-half of the separation between the two half-intensity points of *each* component of the spectrum (referred to as the "half-width").